ENERGY AND ENVIRONMENTAL ANALYSIS OF AN OPEN-LOOP GROUND-WATER HEAT PUMP SYSTEM IN AN URBAN AREA

by

Giorgia BACCINO [a], ***Stefano LO RUSSO*** [b], ***Glenda TADDIA*** [b], ***and Vittorio VERDA*** [a*]

[a] Department of Energy Engineering, Politecnico di Torino, Torino, Italy
[b] Department of Land, Environment and Geo-Engineering, Politecnico di Torino, Torino, Italy

Original scientific paper
UDC: 621.577.2:556.32:620.97
DOI: 10.2298/TSCI1003693B

In this paper a multidisciplinary methodology for analyzing the opportunities for exploitation of open-loop groundwater heat pump is proposed. The approach starts from a model for calculation of a time profile of thermal requirements (heat and domestic hot water). This curve is then coupled with a model of the control system in order to determine the heat pump operation, which includes its energy performances (primary energy consumption) as well as profiles of water discharge to the aquifer in terms of mass flow rate and temperature. Then the thermo-fluid dynamics of the aquifer is performed in order to determine the system impact on the environment as on possible other systems. The application to a case study in the Piedmont region, in Italy, is proposed.
Energy analysis of the system shows that ground-water heat pumps constitute an interesting option in areas with small housing density, where there is not district heating. In comparison with typical heating/cooling systems, environmental benefits are related with reduction in global emissions. These benefits may be significantly enhanced using renewables as the primary energy source to produce electricity. The analysis also shows that possible issues related with the extension of the subsurface thermal plume may arise in the case of massive utilization of this technology.

Key words: *ground water heat pump, energy analysis, environmental analysis*

Introduction

Geothermal heat pumps represent an interesting technology that is expected to contribute significantly to the reduction of primary energy use for heating and cooling and meet the targets set by the European Union. Additional benefits of this technology are related with the integration with intermittent energy resources, in particular wind, and combined heat and power [1, 2].

Among the available heat pump technologies, ground-water heat pumps (GWHP) has potential advantages in terms of energy efficiency and environmental impact, but performances

* Corresponding author; e-mail: vittorio.verda@polito.it

strongly depend on the heating and cooling load, the energy system operation (coefficient of performance – COP, control strategy) and the characteristics of the aquifer. In the case of open loop systems, potential energy associated with water depth is not recovered even if the outlet water is re-injected in the ground, thus this quantity affects the energy required for pumping and must be specifically calculated for the considered site. In addition, the impact on the ground-water temperature in the surrounding area depends on the water mass flow rate extracted to feed the heat pump, the temperature difference, and the natural velocity of water in the aquifer. In particular, the extension of perturbed area is larger as the water velocity increases. This is confirmed by the numerical results obtained in [3] for closed loop heat pumps, when the contribution due to advection is considered in the ground heat exchange. Temperature distribution affects the heat pump efficiency if the perturbed area reaches the extraction well (or the extraction well of other heat pumps installed in the surrounding areas).

Most analyses proposed in the literature are focused on the evaluation of energy efficiency of heat pump systems or their economic aspects (see, for example, [4-9]). In this paper, the overall system effectiveness is evaluated using a multidisciplinary analysis joining together information from energy analysis with hydro-geological analysis. The proposed approach uses three integrated models: (1) a simplified time dependent energy model of the building (including outdoor temperature and sun irradiation), in order to determine heating and cooling load once the control strategy is set; (2) a steady-state model at component level for the heat pump, able to simulate its behavior in off-design conditions; (3) a CFD model of the aquifers able to describe the impact of the heat pump on the ground-water temperature. The model is used to determine the actual energy efficiency of the heat pump system as well as the impact on the area in terms of aquifer level and temperature.

Table 1. Average monthly temperature in Torino

Month	Average air temperature [°C]
January	1.5
February	3.6
March	7.9
April	12.0
May	16.4
June	20.3
July	22.9
August	21.9
September	18.2
October	12.7
November	6.9
December	2.9

Building model and heat pump model

The site under evaluation covers a total area of about 3.600 m^2 (60 m square). The building volume is 18200 m^3 and is located in the urban area of Torino city (see fig. 1), the capital of Piedmont Region, in the north-western area of Italy (geographical co-ordinates 45°04'N, 7°41'E). Relevant climatic data (tab. 1) indicate that the mean annual air temperature is close to 12.5 °C and that the mean monthly temperatures range between 1.5 °C and 22.9 °C.

The building is considered as a single control volume and modeled through the energy equation, which parameters are calculated from simulations performed using a more detailed model, obtained using a commercial software [11]. A simple model can be easily implemented in order to include a realistic control strategy, instead of assuming constant temperature in the rooms. In addition, it can be used in order to convert the energy requirements of the building into the corresponding energy requirements of the air conditioning system, considering also transformations involving change in air humidity.

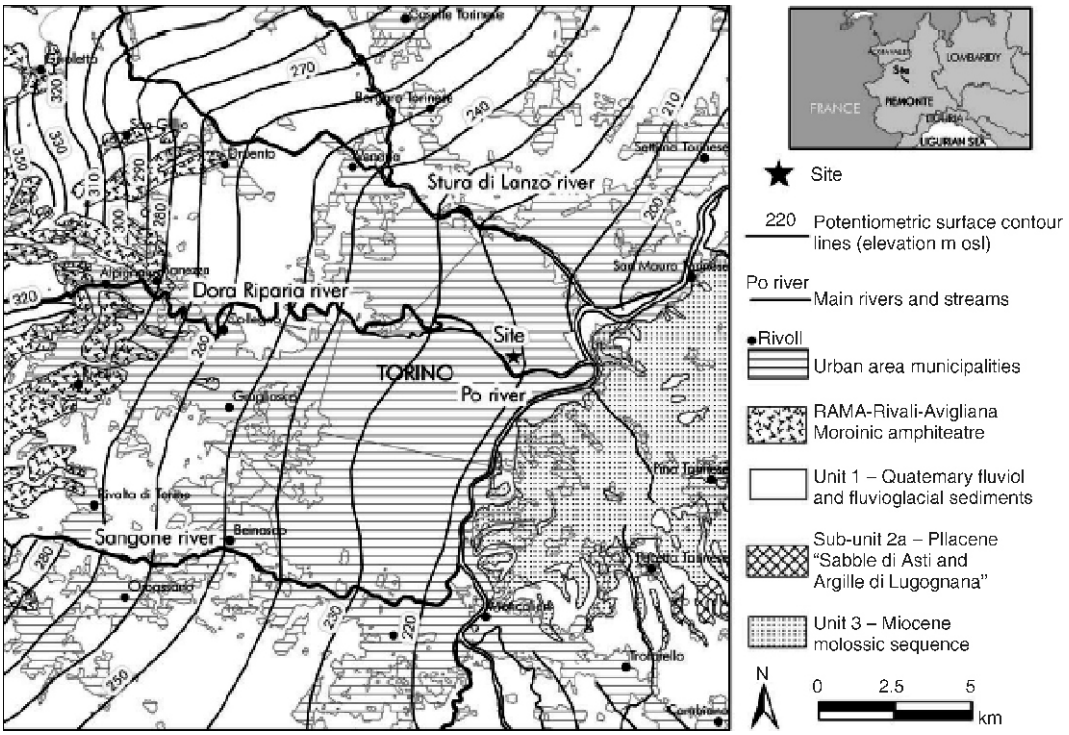

Figure 1. Hydro-geological map of the Turin area and location of the site (modified after [10])

Energy equation for the building is written as:

$$\Phi_{\mathrm{HCS}} \quad a\Phi_{\mathrm{sol}} \quad KV(T \quad T_{\mathrm{e}}) \quad Mc\frac{\mathrm{d}T}{\mathrm{d}t} \tag{1}$$

Φ_{HCS} is the heat flux associated with heating/cooling system. In the case of an air conditioning system this is equal to the difference between inlet and outlet enthalpy flows of the air.

The second term is the net contribution due to the solar radiation: a is the average absorption coefficient of the building and Φ_{sol} is the total radiation over the building plant surface.

The third term accounts for heat transfer through the walls. K is a volumetric heat transfer coefficient, V is the building volume, T – the internal air temperature, and T_{e} – the external air temperature.

Last term accounts for time variation in internal energy, Mc is the heat capacity and $\mathrm{d}T/\mathrm{d}t$ is the time derivative of the internal temperature.

Some simulations are conducted in order to calculate the three parameters: K, Mc, and a.

Volumetric heat transfer has been calculated from simulations in winter conditions, in steady-state and without contribution due to solar radiation:

$$\Phi_{\mathrm{HCS}} - KV(T - T_{\mathrm{e}}) = 0 \tag{2}$$

The calculated value of K is 0.8 W/m^{3}K. This is similar to values obtained from experimental data of a significantly large number of buildings [12].

Thermal capacity Mc has been evaluated considering simulations corresponding with winter and summer nightly cooling when heating/cooling system is shut down:

$$KV(T \quad T_e) \quad Mc\frac{dT}{dt} \tag{3}$$

The calculated value of thermal capacity is $5 \cdot 10^8$ J/K.

The parameter a is not a constant, but it depends on various quantities, as solar radiation, hour of the day, day of the year, *etc*. In addition, errors associated with the model affect the value of this parameter. A neural network model has been used to obtain this value. Four variables have been considered as the input: the radiation on the horizontal plane, the outdoor temperature, the internal temperature (evaluated at the previous time step), and the hour of the day. The neural network is composed by two layers of 15 neurons each: in the first layer the neurons apply a sigmoid function to the inputs, while the second layer is linear. Levenberg-Marquardt algorithm has been used to train the network [13]. To train the network, 1152 values of the input the corresponding values of parameter a and the corresponding output have been used. Figure 2 shows the correlation between known values of parameter a and corresponding values calculated using the neural network; values shown in the figure are non-dimensional.

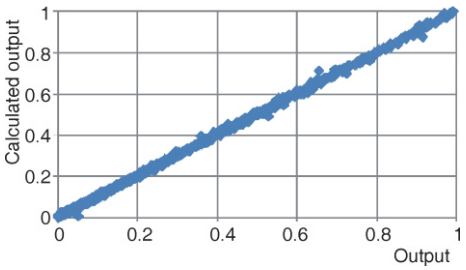

Figure 2. Comparison between absorption coefficients obtained from the detailed model and the neural network model

Concerning the heat pumps (in the building two heat pumps are installed), the model has been built starting from performance data available on data sheets and from measurements on a heat pump system operating in the University. These data are shown in tab. 2, while a schematic of the plant is shown in fig. 3. In fig. 3, the pressure *vs*. enthalpy diagram corresponding with typical summer operation is shown. Working fluid is R134a.

Table 2. Heat pump operation characteristics

Quantity	Value	Quantity	Value
Heating power (heating mode)	370 kW	Pressure drop in the condenser	0.14 bar
Cooling power (cooling mode)	300 kW	Ground-water inlet temperature	15 °C
COP (heating mode)	4.02	Ground-water outlet temperature (heating mode)	5 °C
COP (cooling mode)	7.78	Ground-water outlet temperature (cooling mode)	23 °C
Evaporator superheating grade	4 °C	Evaporation temperature (heating mode)	4.9 °C
Condenser subcooling grade	5 °C	Evaporation temperature (cooling mode)	6.4 °C
Compressor isentropic efficiency	0.75	Condensation temperature (heating mode)	54.4 °C
Pressure drop in the evaporator	0.18 bar	Condensation temperature (cooling mode)	32.7 °C

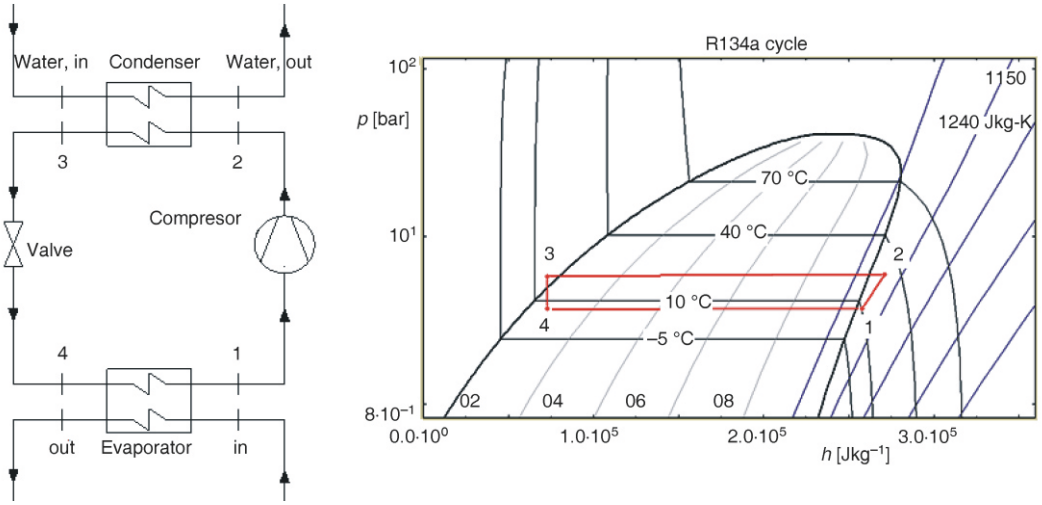

Figure 3. Schematic of the heat pump and *p-h* diagram

The off design model has been generated in the EES environment (Engineering Equation Solver). Condenser and evaporator have been modeled considering constant pressure drops and the effectiveness-NTU method for heat transfer. Constant values for the product of the overall heat transfer coefficient and the heat transfer surface have been assumed (UA = 34.8 kW/K for the condenser, UA = 331.8 kW/K for the evaporator). These values are obtained from operation in design condition, considering a counter-current configuration of the heat exchangers, and are assumed as constant in off-design conditions. The compressor has been modeled considering constant isentropic efficiency. The compressor and the pumps are driven trough inverter, thus the mass flow rates can be varied continuously in off-design.

A control strategy for the heating and cooling system is set to model off-design conditions. During the night the system is off. During the day, indoor temperature is kept between 19.5 °C and 20.5 °C in winter and between 26 °C and 27 °C in summer. As for the heat pump, it operates keeping the superheating grade in the evaporator and the subcooling grade in the condenser as constant.

System model results

Figure 4 shows the internal temperature (T) and external temperature (*Test*) in a typical winter day.

The heating system is started at full load at 6:30. Set point temperature is reached at about 10:00, then the system operates at part load (a single heat pump at full load) for 1.5 hours and then is stopped. After 2.5 hours a single heat pump is started at full load for 2.5 hours and then stopped for 1.5 hours. Finally a single heat

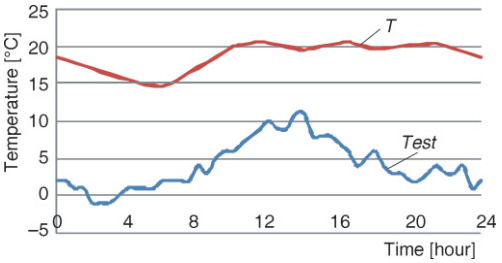

Figure 4. Temperatures in a typical winter day

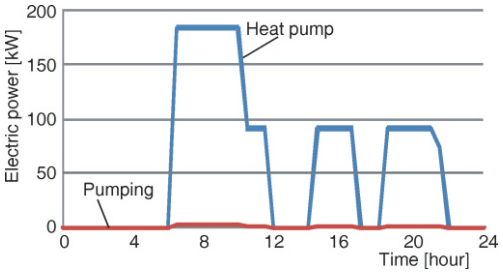

Figure 5. Electric power for the heat pumps and pumping in a winter day

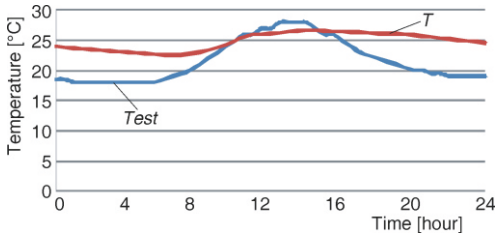

Figure 6. Temperatures in a typical summer day

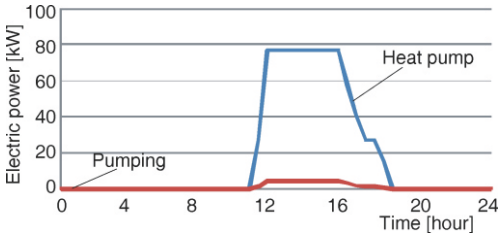

Figure 7. Electric power for the heat pumps and pumping in a summer day

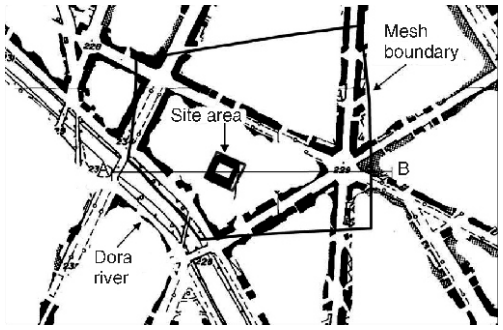

Figure 8. Plan view of the site overlain onto the simplified topographical map

pump is started at full load for 3.5 hours and then stopped until next morning. Figure 5 shows the electric power required during the day. The contribution due to pumping is also shown in the figure. In this particular case, the latter is about 2.5% of the electric power required by the two heat pumps. This means that the net COP reduces to about 3.92 in design conditions.

The internal and external temperatures in a typical summer day are shown in fig. 6. In this case the heat pump system is started at 11:00 at half load and then turned at full load at 12:00 until 15:30. Then the system load is slightly reduced until it is tuned off at 18:30.

The corresponding electricity consumption is shown in fig. 7. As shown in the next paragraphs the extraction well temperature is not affected by the hot water re-injection in this case. If a different control strategy is considered the inlet temperature might increase which would affect the heat pump performances.

When pumping is considered in the net COP, it drops to about 7.3, which is significantly less than the nominal value (7.8).

Site description

Torino urban area is mainly developed on the outwash plain constituted by several glaciofluvial coalescing fans connected to the Pleistocene-Holocene expansion phases of the Susa glacier. The plain extends between the external Rivoli-Avigliana Morainic Amphitheatre (RAMA – Susa Glacier) on the west side and the Torino hill on the east. The plant considered in this work is located near the Dora Riparia river (see fig. 8), which dissects the plain and discharge in the main draining Po river that flows towards N-E along the western border of Torino hill.

The outwash plain substrate outcrops in correspondence of the Torino hill and is constituted by a Cenozoic terrigenous marine succession deposed in an episutural basin (according to [14]) (see fig. 1). As a result of a complex

Pliocene-Holocene evolution characterized by the deposition of continental sediments related to the dynamic evolution of the Plio-Pleistocene "Villafranchian" glaciolacustrine facies [15] and the Pleistocene-Holocene expansion phases of the Susa glacier, the urban area plain geological setting is characterized by a strong geographical anisotropy.

The hydro-geological setting is known with a high degree of confidence due to the large number of wells drilled in the urban area [16]. The study area downhole log data indicate the presence of two lithologic zones with distinct hydraulic properties.

Unit 1 – (Middle Pleistocene-Holocene; from the surface to 29 m depth). Continental alluvial cover composed mainly of coarse gravel and sandy sediments (locally cemented) derived from alluvial fans aggraded by the alpine rivers down streaming towards east. The Unit 1 bottom (erosional surface) gently dips (0.5%) towards north-east overlaying Unit 2.

Unit 2 – (Early Pliocene-Middle Pleistocene; from 29 m depth). Originally deposited in a shallow marine environment and traditionally defined as Sabbie di Asti and/or Argille di Lugagnano is mainly composed of fossiliferous sandy-clayey layers with subordinate fine gravely and coarse sandy marine layers or by quartz-micaceous sands with no fossil evidences. In other portions of the urban area it highlights heteropic relationships with fluvio-lacustrine facies usually referred to as the "Villafranchian" consisting of fine-grained sediments (sand, silt, and clay with interbedded gravel) divided into several sedimentary bodies [15]. The top of the Unit 2 was eroded away and covered by the alluvial deposits of Unit 1.

Characterization of the aquifers

In order to model ground-water flow and heat transport in the subsurface linked to the GWHP, an accurate characterization of the hydro-geological and hydrodynamic properties is required. This information allows one to determine the sustainable well pumping rates and the thermal plumes connected to the injected (warm or cool) ground-water. The vulnerability to pollution of the different aquifers must also be considered. The characterization is focused on the Unit 1 aquifer, which is considered viable for the GWHP plant, especially in terms of the energy costs of pumping and injection. Simulations involving the utilization of ground-water indicate that Unit 1 is sufficient for providing ground-water and related energy needs.

The unconfined aquifer that extends over the entire urban plain, including the location of the investigated site, is hydraulically connected to the main surface water drainage network in the area (*i. e.* the Dora river). This aquifer is hosted in Unit 1 and is quite vulnerable to pollution because of its shallow depth and the direct connection with the surface water drainage network. The potentiometric surface, 6 m below ground level, shows a W-to-E gradient of 0.4%. The saturated thickness of the unconfined aquifer is about 23 m.

A 29-m deep pumping well has been drilled in the centre of the site in order to provide an adequate amount of ground-water for the GWHP plant. The ground-water temperature is 15.0 °C. First, a step drawdown well test has been performed to evaluate the sustainable long-term pumping rate and characterize the hydro-geological properties of the aquifer in Unit 1. The test data yielded a sustainable pumping rate of 18 L/s, a transmissivity (T_1) of 5.61 10^{-3} m^2/s. The hydraulic conductivity (K_1 = 2.4 10^{-4} m/s) has been calculated assuming an average saturated thickness of 23 m. The storativity (S_1) has been assumed 0.106 as a result of a constant-rate pumping test set out in the same Unit 1 [17].

An unconfined aquifer system occurs in the Unit 2. It exhibit only a moderate intrinsic vulnerability to pollution, due mainly to its depth (on average, the top of Unit 2 is at 29-30 m

depth). Only damaged or improperly constructed wells, connecting Units 1 and 2, cause contamination of this deep aquifer. Due to the local absence of confining impermeable layers near the site, water levels in wells completed in this Unit 2 system are coincident with those measured in the overlaying Unit 1. The undisturbed ground-water temperature for Unit 2, as measured in productive wells 1.0 km from the site, is the same as that of Unit 1 (15.0 °C). The hydraulic properties of the Unit 2 aquifer system, useful for the modelling phase, have been determined based on three constant-rate aquifer tests [18]. These tests gave the following average hydraulic parameters: transmissivity $T_2 = 7.88\ 10^{-3}$ m^2/s and storativity $S_2 = 7.22\ 10^{-4}$. Based on the lithology of the aquifers, the effective porosity is assumed to be 0.20.

Modeling study of the aquifer

To evaluate the environmental effects of a GWHP system and to delineate the optimal configuration of the ground-water injection well, a modeling study has been performed using the finite-element FEFLOW® package developed by Diersch [19]. Of particular interest with regard to the model simulations is the areal extent and sustainability of the subsurface thermal plume developed around the injection well at the maximum flow conditions set out in the summer (June-September) during cooling operations. To evaluate the hydraulic sustainability of the ground-water production-injection system and the resulting temperature effects (extent of the thermal plume), numerical modeling studies have been performed to compare three different scenarios, as detailed in tab. 3. Two scenarios (case A and B) corresponds to possible summer conditions, whilst case C corresponds to winter conditions. Case A presents variable injection temperatures (from 19.5 to 23 °C), whilst in case B and case C a constant value in the injected ground-water is considered (23 and 10 °C, respectively).

All these scenarios involve ground-water extraction only from the aquifer of Unit 1 with the waste-water (water that had circulated through the heat exchangers) being fully injected into the same ground-water system. Fortunately, it should be noted that a subsurface artificial channel at the site, can handle the maximum amount of water used by the heat pumps, both in terms of quantity and temperature. Therefore an actual working hypothesis for the GWHP plant can be represented by the discharge of ground-water thermally treated directly in this surface water drainage system avoiding subsurface thermal plume development. In this case, it would be sufficient to verify the aquifer subsurface sustainability of withdrawals and not to determine the thermal effects associated with warmer (or cooler) discharge. Moreover, to preserve ground-water quality and chemistry, the current Italian national laws and regulations [20] prohibit the injection of ground-water derived from one aquifer into another. Therefore, the case of ground-water withdrawal from Unit 1 and injection into Unit 2 (or *vice-versa*) has not be considered.

A conceptual model with two layers has been simulated using physical properties appropriate to the hydro-geology of the formations. Layer 1 represents the unconfined aquifer in Unit 1, Layer 2 correspond to the Unit 2 (see fig. 9). The distribution of the different layers in the model area is determined from topographic elevation data for the different geological units as listed in the regional authority database [16]. The initial ground-water temperature for Units 1 and 2 was set at 15.0 °C as experimentally determined. The volumetric heat capacity and heat conductivity for water and rock were set equal to the default parameters in the FEFLOW model, as listed in tab. 3. Considering the level of uncertainty associated with the lithology, these values are consistent with Japanese Society of Thermophysical Properties.

Table 3. Open-loop ground-water heat pump system daily scenarios

Time	Summer (cooling) Case A		Summer (cooling) Case B		Winter (heating) Case C	
	Withdrawal rate [Ls^{-1}]	Injection temperature [C°]	Withdrawal rate [Ls^{-1}]	Injection temperature [C°]	Withdrawal rate [Ls^{-1}]	Injection temperature [C°]
0-1 a.m.	0	0	0	0	0	0
1-2	0	0	0	0	0	0
2-3	0	0	0	0	0	0
3-4	0	0	0	0	0	0
4-5	0	0	0	0	0	0
5-6	0	0	0	0	17.7	10.0
6-7	0	0	0	0	17.7	10.0
7-8	0	0	0	0	17.7	10.0
8-9	0	0	0	0	17.7	10.0
9-10	0	0	0	0	17.7	10.0
10-11	15.9	19.5	9.0	23.0	17.7	10.0
11-12	17.9	23.0	17.9	23.0	0	0
12-1 p.m.	17.9	23.0	17.9	23.0	0	0
1-2	17.9	23.0	17.9	23.0	0	0
2-3	17.9	23.0	17.9	23.0	17.7	10.0
3-4	17.1	22.0	14.9	23.0	17.7	10.0
4-5	15.9	19.5	9.0	23.0	0	0
5-6	10.6	19.5	6.0	23.0	0	0
6-7	0	0	0	0	17.7	10.0
7-8	0	0	0	0	17.7	10.0
8-9	0	0	0	0	17.7	10.0
9-10	0	0	0	0	7.2	10.0
10-11	0	0	0	0	0	0
11-12	0	0	0	0	0	0

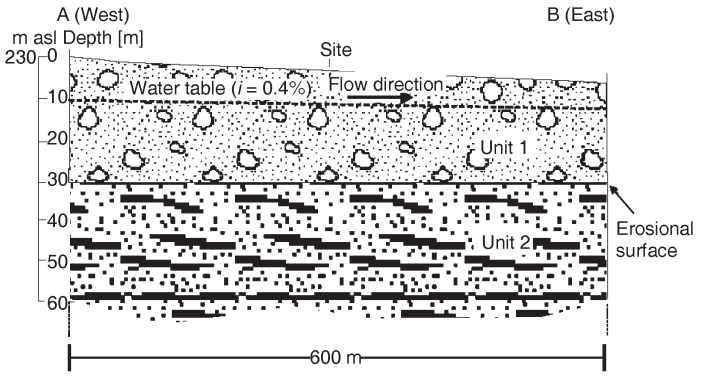

Figure 9. Schematic hydro--geological cross-section of the site under study (see Figure 9 for location); *i* – gradient of potentiometric surface

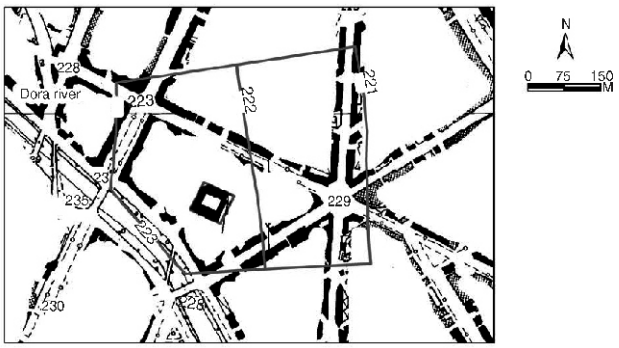

Figure 10. Potentiometric surface for the Unit 1 unconfined aquifer under undisturbed conditions (in metres above mean sea level, m asl); contour spacing: 1 m

A plan view of the area covered by the computational grid (about 205.000 m^2; 36.584 elements and 18.541 nodes) is shown in fig. 8. The horizontal dimensions of the model grid are 540 m (W-E) and 445 m (N-S). The model was assumed to be closed to fluid flow at its top and bottom. Rainfall infiltration was not included in the calculations due to a lack of measured infiltration data. Instead, the recharge to the system was simulated by fixing ground-water levels on the outer boundaries (Dirichlet conditions). These levels have been determined by initially calibrating the model against the steady-state ground-water heads obtained from a potentiometric surface map [10] (see fig. 10)

The most important mechanisms of heat transport in a saturated porous medium with a moving fluid, such as the saturated levels in an aquifer system, are convection and hydrodynamic thermodispersion. Thus, the resulting geometry of the thermal plume in the aquifer is influenced by the longitudinal and transverse thermodispersivity values as highlighted in [17]. Preliminarily, a sensitivity analysis of longitudinal and transverse thermodispersivity for the case A has been performed to compare the subsurface thermal plumes resultant varying these parameters. Computed differences in the thermal plumes extents have been very slight (lower than 0.1 m) thus, the FEFLOW model default values for thermodispersivity (5 m and 0.5 m for α_L and α_T, respectively) have been used for all simulations (case A, B, and C).

Modeling run assuming transient conditions for ground-water flow and for heat transport in order to correctly compute heat dispersion around the injection well. In particular we simulated the cyclic repetition (7-days long) of the daily withdrawals (and respective injections) and ground-water temperatures showed in tab. 4. Appropriate FEFLOW time-varying functions for discharge and temperatures have been implemented for each case. Transient conditions modeling are time-consuming but permits to improve the goodness of the estimate for the actual thermal dispersion around the injection well respect steady-state ground-water conditions. In fact, the steady-state conditions have to take into account withdrawals and temperature values daily (or monthly) averaged and thus can overestimate (or underestimate) the actual impact on the aquifers in terms of potentiometric surface changes and thermal plumes dimension. On the opposite, transient conditions can consider variable weather and the night-day

Table 4. Thermal parameter used for FEFLOW modeling

Quantity	Layers 1 and 2
Volumetric heat capacity of the fluid [10^6Jm^{-3}K^{-1}]	4.2
Volumetric heat capacity of the solid [10^6Jm^{-3}K^{-1}]	2.52
Heat conductivity of the fluid [Jm^{-1}s^{-1}K^{-1}]	0.65
Heat conductivity of the solid [Jm^{-1}s^{-1}K^{-1}]	3
Longitudinal dispersivity [m]	5
Transverse dispersivity [m]	0.5

cycles that influence air temperature, insulation, and changes in the buildings' energy needs because of varying ventilation rates.

Results and discussion

Simulations demonstrated the feasibility of Unit 1 supplying the required maximum withdrawals in all cases considered. The injection well has been located in the N-E corner of the site to optimize the distance from the extraction well and thus reduce the hydraulic and thermal interferences between simultaneous ground-water withdrawal and injection. Figures 11(1) and 11(2) show the results for thermal plume developed in case A and B, respectively, while fig. 12 shows the subsurface effects in the winter simulation (case C). Figure 11(3) highlights a comparison between the maximum extent of the summer thermal plumes for case A and B illustrated by the 16 °C isotherm.

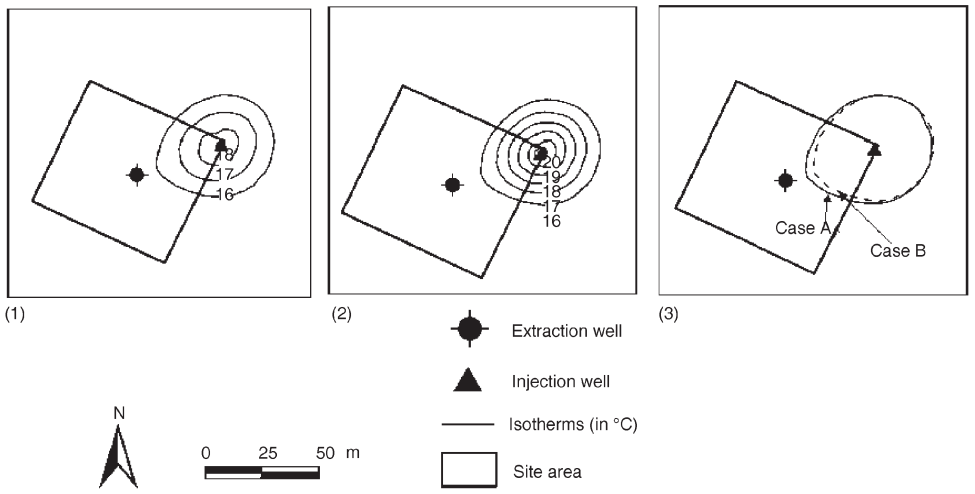

Figure 11. Study area. Temperatures [ºC] in the Unit 1 unconfined aquifer after 7 days of injecting warmer water
(1) Isotherms for case A; (2) Isotherms for case B; (3) Location of the 16.0 °C isotherms in the case A and case B; contour spacing: 1 ºC

In the three scenarios the resulting pressure decline and consequent alteration in the potentiometric surfaces would not significantly interfere with existing off site wells and with the extraction well in the middle of the site. Moreover, the thermal plumes would mostly extend to an internal area respect the site boundaries. On the opposite, after a 7-days long transient simulation the ground-water temperature in the extrac-

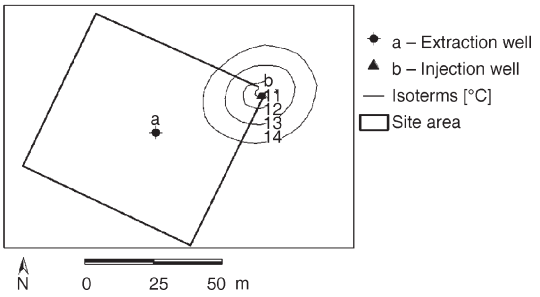

Figure 12. Study area; Case C; Temperatures [ºC] in the Unit 1 unconfined aquifer after 7 days of injecting cooler water; contour spacing: 1 ºC

tion well pass from the initial (15 °C) to 15.30 °C (case A), 15.14 °C (case B), and 14.91 (case C). Despite their slight absolute values, these variations probably highlight an harmful subsurface phenomenon consisting in a closed loop between extracted and injected ground-water probably due to the insufficient wells distance. Thus, this evidences could represent a limit for the development of such system and could induce choosing to discharge the waste-water in the subsurface channel present at the site.

Figure 11(3) highlights a wider extent of the thermal plume for the case A respect the case B. This evidence suggests that it could be more convenient to reduce the withdrawals and maximize the ΔT in the heat pump exchangers to reduce the subsurface environmental impacts from the operation of the GWHP system. However, considering the slight differences, the best compromise should be reached also considering the total (electric) energy demand for the total system (wells and heat pump).

The winter simulation (case C) confirms the smaller dimensions of the (cool) thermal plume in the aquifer and a relatively reduced alteration of the potentiometric surface due to lower ground-water injection (and production) rates.

Conclusions

This study has demonstrated the feasibility of a GWHP plant providing the heating and cooling needs of the new building complex.

The hydro-geologic conditions of the site would support the exploitation scenarios. The simulations demonstrate the possibility of using Unit 1 to provide the required rates of ground-water extraction for GWHP system being considered for the air-conditioning project.

Major problems have been highlighted by the simulated temperature in the extraction well at the end of the transient simulations performed (7-days). The variations respect the initial temperature underline the difficult for the aquifer to recover thermally between repeated daily cycles, without avoiding the risk of a long-term drift in temperatures in the production and injection regions during a season (both summer and winter) that might eventually necessitate the abandonment of the project. Due to the logistic condition of the site this risk could not be avoided increasing the distance between injection and extraction well but only opting for a waste-water discharge by means of the artificial channel present at the site.

However this study indicates that the aquifer at the site could provide the thermal energy required by GWHP system without causing a significant thermal impact on the underground.

Concerning the energy performances, the primary energy consumption of the heat pump system unit in winter operation is about 0.6 kJ per each kJ of heat supplied to the user. This amount is much smaller than condensing boilers, but it is larger than district heating system, which is available in a large area of the town. In the case of district heating, in fact, this indicator is about 0.5 kJ/kJ [21]. Nevertheless, district heating becomes less efficient from the primary energy consumption viewpoint when small buildings are considered, or when the buildings are far from the thermal plant or in areas with small habitant density. In this case ground-water heat pumps constitute a valid alternative in terms of primary energy consumption and CO_2 emissions. In the case of summer cooling, which is becoming an issue as high picks in electricity consumptions occur, this option is absolutely interesting as it is characterized by high values of COP.

The integration of the energy analysis and the hydro-geological analysis has proven to be an effective approach to correctly determine the energy performance of a GWHP system, in particular when several applications are planned in the same area, to check the control strategy in order to avoid shortcuts (in particular, extraction of re-injected hot water in summer) and to evaluate the environmental impact of the system.

This tool is currently used by the working group to analyze a complete year operation of the system.

Acknowledgments

The authors thank Dr. Gianfranco Gardenghi and the environmental authority of the Piedmont Region for their assistance during the field survey and for allowing publication of the data. This study was partially supported by Piedmont Region.

Nomenclature

a – average absorption coefficient, [–]
K – volumetric heat loss coefficient, [kWm^{-3}K^{-1}]
Mc – thermal capacity of the building, [kJK^{-1}]
T – indoor temperature, [°C]
T_e – external temperature, [°C]
V – building volume, [m^3]
Φ_{HCS} – heat flux from the heating system, [kW]
Φ_{sol} – inlet heat flux from the sun, [kW]

References

[1] Blarke, B. L., Lund, H., The Effectiveness of Storage and Relocation Options in Renewable Energy Systems, *Renewable Energy, 33* (2008), 7, pp. 1499-1507
[2] Ozgener, O., Use of Solar Assisted Geothermal Heat Pump and Small Wind Turbine Systems for Heating Agricultural and Residential Buildings, *Energy, 35* (2010), 1, pp. 262-268
[3] Fan, R., *et. al*., A Study on the Performance of a Geothermal Heat Exchanger under Coupled Heat Conduction and Groundwater Advection, *Energy, 32* (2007), 11, pp. 2199-2209
[4] Hepbaslia, A., Balta, M. T., A Study on Modeling and Performance Assessment of a Heat Pump System for Utilizing Low Temperature Geothermal Resources in Buildings, *Building and Environment, 42* (2007), 10, pp. 3747-3756
[5] Zhao, L., *et. al.*, Theoretical and Basic Experimental Analysis on Load Adjustment of Geothermal Heat Pump Systems, *Energy Conversion and Management, 44* (2003), 1, pp.1-9
[6] Ozgener, O., Hepbasli, A., Modeling and Performance Evaluation of Ground Source (Geothermal) Heat Pump Systems, *Energy and Buildings, 39* (2007), 1, pp. 66-75
[7] Kara, Y. A., Yuksel, B., Evaluation of Low Temperature Geothermal Energy through the Use of Heat Pump, *Energy Conversion and Management, 42* (2001), 6, pp. 773-781
[8] Smolen, S., Budnik-Rodz, M., Technical and Economic Aspects of Waste Heat Utilization, *Thermal Science, 11* (2007), 3, pp. 165-172
[9] Blarke, M. B., Lund, H., Large-Scale Heat Pumps in Sustainable Energy Systems: System and Project Perspectives, *Thermal Science, 11* (2007), 3, pp. 143-152
[10] Civita, M., Lo Russo, S., Vigna, B., Hydrogeological Sketch Map of Piemonte (NW Italy) 1:250.000, *Proceedings*, 32nd International Geological Congress (32IGC), 2004, Florence, Italy
[11] Giordano, F., Energy Analysis of a Groundwater Heat Pump System (in Italian), M. Sc. thesis, Politecnico di Torino, Italy, 2009
[12] Verda, V., Ciano, C., Procedures for the Search of the Optimal Configuration of District Heating Networks, *The International Journal of Thermodynamics, 8* (2005), 3, pp. 143-154
[13] Hagan, M. T., Menhaj, M. B., Training Feed-Forward Networks with the Marquardt Algorithm, *IEEE Transactions on Neural Networks, 5* (1994), 6, pp. 989-993

[14] Bally, A. W., Snelson, S., Realms of Subsidence, in: Facts and Principles of World Petroleum Occurrence (Ed. D. Miall), *Canadian Society of Petroleum Geologists Memoir* 6, 1980, pp. 9-94
[15] Carraro, F., Moscariello, A., Review of the Villafranchian in Villafranca d'Asti (in Italian), AIQUA-CNR, Tefrocronologia, 1994, Rome, Italy, pp. 126-127
[16] ***., Regione Piemonte, Water Protection Plan 2007, D.C.R.n. 117-10731, Turin, Italy (in Italian), http://www.regione.piemonte.it/acqua/pianoditut
[17] Lo Russo, S., Civita, M.V., Open-Loop Groundwater Heat Pumps Development for Large Buildings: A Case Study, *Geothermics, 3* (2009), 3, pp. 335-345
[18] Di Molfetta, A., Cordero, P., Sethi, R., Interference between Road Network and Groundwater Resources. *Proceedings,* 5th International Congress on Energy, Environment and Technological Innovation EETI*,* 2004, Rio de Janeiro, Brazil, pp. 1-7
[19] Diersch, H.-J. G., Reference Manual for FEFLOW, 2005, http://www.feflow.info
[20] ***, Repubblica Italiana, Environmental Standards (in Italian), *Gazzetta Ufficiale, 88* (2006), Supplemento Ordinario No. 96, http://www.parlamento.it/leggi/deleghe/06152dl.htm
[21] Verda, V, Fausone, S., Exergoeconomic Evaluation of District Heating Systems, *Proceedings*, 3rd International Conference on Energy Sustainability, ASME 2009 (2009), San Francisco, Cal., USA, paper ES20009-90351, pp. 1-7

Paper submitted: November 24, 2009
Paper revised: April 1, 2010
Paper accepted: April 14, 2010